Proceedings of the
International Conference on Mechanical Engineering 2005
(ICME2005) 28- 30 December 2005, Dhaka, Bangladesh

ICME05-FL-05

EFFECT OF SURFACE ROUGHNESS ON TURBULENT TRANSONIC FLOW AROUND A RAE-2822 AIRFOIL

J. E. Michael and M.A.R. Sharif

Aerospace Engineering and Mechanics Department, Tuscaloosa, Alabama, 35487-0280, USA

ABSTRACT

The aerodynamic effects of surface roughness on the RAE-2822 transonic airfoil are explored using the FLUENT CFD code. The parameters of the investigation are the free-stream Mach number, angle of attack, and surface roughness height. The k-ω turbulence model with enhanced wall treatment is used in the computation. The pressure coefficient and skin friction coefficient distributions around the airfoil and lift and drag on the airfoil are computed for a range of the aforementioned flow parameters. Results show that roughness has a significant effect on lift and viscous drag. The pressure drag, which is an order of magnitude larger than the viscous drag, is rather insensitive to the surface roughness. Upward lift is found to diminish rapidly as roughness height grows. Finally, the boundary layer thickens and the shock on the upper surface moves upstream along the chord as roughness increases.

Keywords: Transonic flow, Shock/boundary layer interaction, RAE-2822 airfoil, Surface roughness.

1. INTRODUCTION

When a subsonic flow above a critical Mach number is locally accelerated over a curved surface into a supersonic flow which is subsequently terminated by a shock, the flow is designated as transonic flow. The incident shock interacts with the boundary layer and produces a very complicated flow behavior called Shock-Boundary Layer Interaction (SBLI) whose analysis and understanding is rather complex. In many practical high-speed flow problems, the SBLI leads to detrimental flow features such as adverse pressure losses, increased drag, and flow alteration/distortion.

The study of transonic flow around an airfoil is particularly important because a large number of military and commercial aircraft operate within the range, which is roughly between Mach 0.7 to 0.9. Although the aircraft or free stream Mach number is subsonic, the flow over the airfoil reaches supersonic speeds and thus transonic shock is produced.

There have been many studies conducted in the past on transonic flow over airfoils. Ahmed and Tannehill [1] computed flow over the RAE-2822 airfoil with a nonequilibrium turbulence model. Anderson and Bonhaus [2] calculated the flow over the RAE-2822 airfoil to validate their implicit upwind algorithm on unstructured grids. Jiang et al. [3] and Lien and Kalitzin [4] did numerical analysis of transonic flow over the same airfoil using various turbulence models. All of these computations are done for two-dimensional airfoil models. Garbaruk et al. [5] performed three-dimensional computations for numerical study of wind-tunnel wall effects on transonic airfoil flow. The aforementioned computations are done for smooth airfoil surfaces. Very few studies on the effect of surface roughness on transonic flow over airfoils are available in the literature. Roughness is present to some extent on all aircraft and can be caused by a number of factors, including but not limited to the defects in workmanship, dirt, natural material roughness, and surface deterioration due to age or impact damage. Cebeci [6] has examined the effects of roughness due to ice formation near the leading edge of the airfoil. Mendonca and Sharif [7] investigated the surface roughness effects on transonic flow over a circular arc bump in a channel.

Computation of SBLI on smooth surfaces is very challenging by itself due to the deficiency of the available turbulence models. Another level of complexity arises if the surface roughness is incorporated into the model. Very little progress has been achieved in modeling turbulence over rough surfaces. General practice is to use the wall function and calculate the near wall velocity using the log-law for rough surfaces. Recent studies found that the law of the wall does not apply in flows with strong pressure gradients and separation where near wall turbulence models should be employed. The ω based models with near wall treatment have the unique feature that the value of ω at the surface is specified as a function of the surface roughness height.

In this study the aerodynamic effects of surface roughness on the RAE-2822 transonic airfoil are investigated numerically. The roughness in this investigation is applied evenly to the entire surface of the airfoil and the roughness type is the uniform sand-grain

roughness. The parameters of computation are the freestream Mach number, M, the angle of attack, α, and the average surface roughness height k_s. The pressure coefficient and skin friction coefficient distributions around the airfoil and drag and lift on the airfoil are computed for a range of the aforementioned flow parameters and the results are presented.

2. COMPUTATIONAL DETAILS

The computations are performed using the FLUENT CFD code. The *k-ω* turbulence model with enhanced wall treatment and options for transitional flows, compressibility effects, and shear flow corrections, as implemented in the FLUENT code, is used in the computation. The $k-\omega$ model is chosen because of the aforementioned convenience of incorporating the roughness in the computation through the specification of ω at the wall in terms of the equivalent sand-grain roughness height. A 270×45 mesh with clustering towards the airfoil surface, shown in Fig. 1, is created around the RAE-2822 airfoil using the GAMBIT pre-processor. This grid distribution is chosen after some grid refinement study and examining the convergence of the pressure coefficient distribution plot around the airfoil with grid refinement. The solutions are allowed to iterate until they converge with normalized residuals dropping below 10^{-5}, usually after 1500 iterations. Roughness is applied to the airfoil surface within FLUENT with a roughness constant of 0.5. The free stream fluid density is specified as 1.176673 kg/m^3.

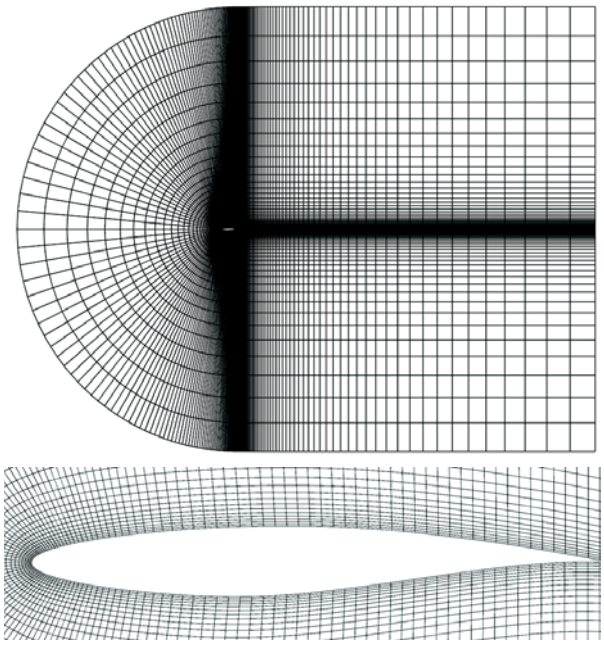

Fig 1. The grid system; top – full domain, bottom – close up around the airfoil.

No slip boundary conditions are applied on the airfoil surface while the pressure-far-field boundary conditions are applied on the far field boundaries around the airfoil. The far-field boundaries are placed at more than 30 chord lengths away from the airfoil so that the effect of the boundary on the near-field flow is insignificant. The values of ω at the airfoil surface are specified as [8]

$$\omega|_{wall} = \left(u_\tau^2 / \nu\right) S_R \tag{1}$$

where u_τ is the shear velocity at the surface, ν is the kinematic viscosity of air, and S_R is a roughness factor specified in terms of the non-dimensional roughness height $k_s^+ = k_s u_\tau / \nu$ as

$$S_R = \begin{cases} \left(50/k_s^+\right)^2, & \text{if } k_s^+ < 25 \\ 100/k_s^+, & \text{if } k_s^+ \geq 25 \end{cases} \tag{2}$$

A validation exercise is conducted by computing the flow field around the airfoil with smooth surface at an angle of attack of 3.19˚ in a free stream Mach number of M = 0.745 and Reynolds number Re = 2.7 × 10^6. Fig. 2 shows the comparison of the predicted pressure coefficient distribution with the experimental results obtained by Cook et al. [9]. Overall the prediction closely coincides with the experimental data even though the predicted shock location is further downstream than it is in reality. Note that along the entire lower surface and downstream of the shock on the upper surface, the prediction is quite accurate.

3. RESULTS AND DISCUSSION

Computations are done for freestream Mach numbers of 0.7, 0.75, 0.8, 0.85, and 0.9. At each free stream Mach number the angle of attack is varied as 0°, 1°, 2°, and 3°. For each of these combinations the sand grain surface roughness height is varied as 0, 0.5, 1, 1.5, and 2 mm. Thus a total of 100 simulations are performed with various combinations of the flow and geometric parameters mentioned above.

The contours of the pressure field around the airfoil for a representative Mach number of 0.8 and angle of attack of 2° are shown in Fig. 3 for smooth ($k_s = 0$) and rough ($k_s = 1\,\text{mm}$) surface cases, respectively. The computation successfully captures the formation of the shocks. The appearance of the shocks on both upper and lower surfaces is observed at this freestream Mach number and angle of attack. The effect of surface roughness is not clearly discernible from these contour plots except the upstream movement of the shock at the upper surface as the roughness height increases. It will be clearly visible in subsequent plots of pressure coefficients and skin friction coefficients on the airfoil surface.

Close up view of the streamtrace plot near the trailing edge of the airfoil for the above case are shown in Fig. 4 which depict the formation of small recirculation bubbles at the upper surface near the trailing edge indicating flow separation. The bubble is noticed to be moving downstream with increasing roughness.

The variation of the pressure coefficient, C_p, along the upper and lower surfaces of the airfoil at a Mach number of 0.8 and at an angle of attack of 2° for various surface roughness heights are shown in Fig. 5 as a

representative case. The effect of surface roughness is clearly discernible from these plots in terms of the movement of the shock location. At the upper surface the shock moves upstream while at the lower surface it moves downstream with increasing roughness height.

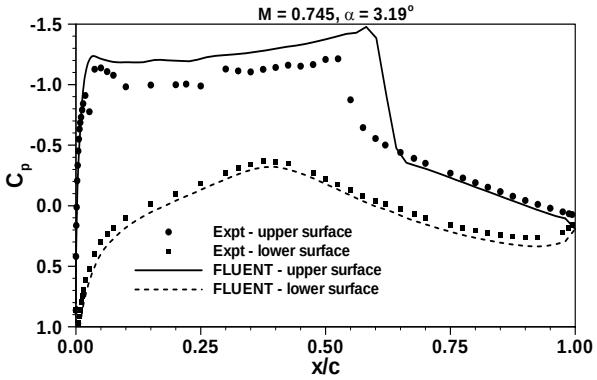

Fig 2. Predicted pressure coefficient distribution along the top and bottom surfaces of the airfoil compared to experimental results.

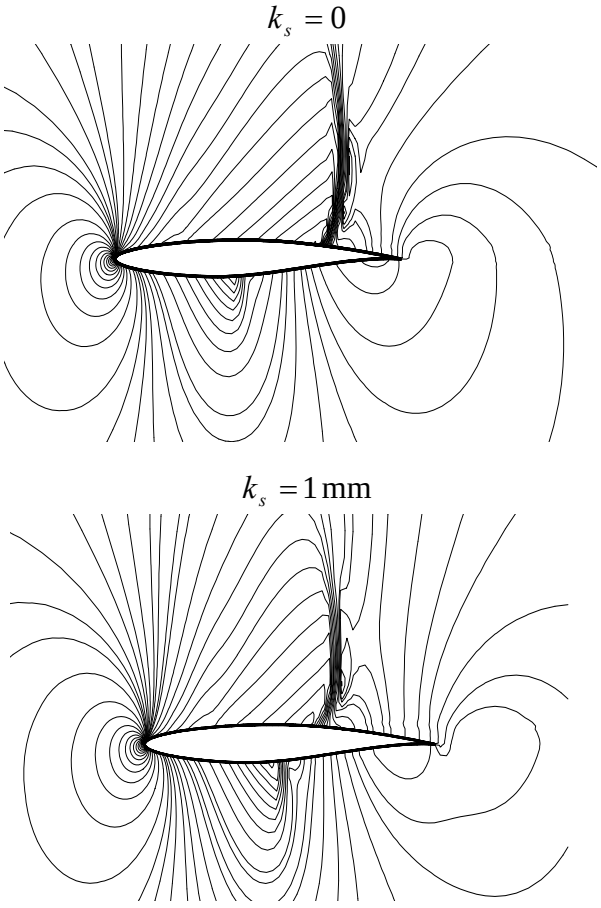

Fig 3. Contour plot of the pressure field around the airfoil for M = 0.8 and α = 2°.

The coefficient of lift, C_L, is a quantity of high importance in the airfoil performance. The effect of surface roughness on the lift coefficient for the RAE-2822 airfoil has also been investigated in this study. Plots for the variation of the lift coefficient with surface roughness at various freestream Mach numbers at a representative angle of attack of 2° is shown Fig. 6. It is observed from this plot that the lift coefficient falls monotonically with increasing surface roughness. The lift coefficient drops quickly up to a roughness height of 0.5 mm and then the decrease is milder for higher roughness heights. At M = 0.9, the lift coefficient becomes almost zero at higher roughness heights indicating an operational problem at this Mach number. The decrease of the lift coefficient is linked with the pressure variation along the airfoil surface and the upstream shifting of the shock location at the upper surface and downstream shifting of the shock at the lower surface.

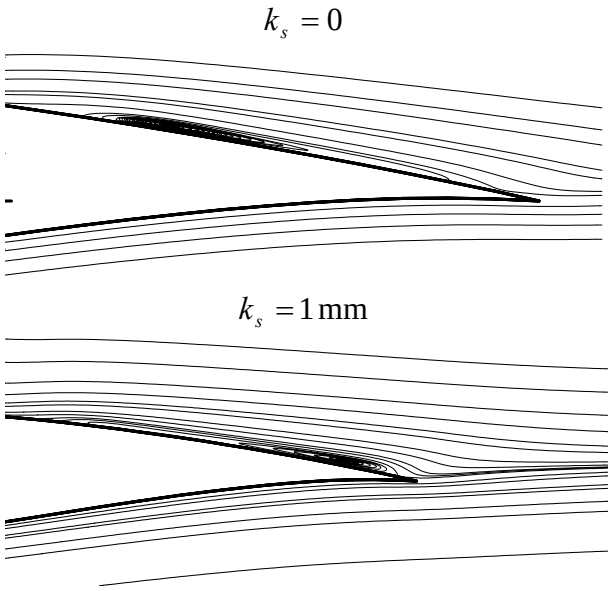

Fig 4. Close up view of the streamtrace plot near the trailing edge of the airfoil for M = 0.8 and α = 2°.

Another important quantity in airfoil performance study is the drag and drag coefficient. The drag mainly arises from two sources; (i) due to the viscous friction at the airfoil surface which is known as the viscous drag, and (ii) because of the pressure differences due to the airfoil geometry, flow separation, and shock formation which is known as the pressure or form drag. In the case of a transonic airfoil both types of drag are affected by the change in surface roughness due to the associated movement of the shock location and the separation bubble and change in the surface friction characteristic. For this reason the effects of surface roughness on the airfoil drag has also been investigated in this study. The viscous friction drag is directly related to the skin friction coefficient, c_f, defined as $\tau_w/(\rho_\infty U_\infty^2/2)$ where τ_w is the shear stress at the airfoil surface and ρ_∞ and U_∞ are the free stream density and velocity, respectively. Representative plots for the variation of the skin friction coefficient on the airfoil surface for M = 0.8 at an angle of attack of 2° is shown in Fig. 7. The values of c_f increase rapidly near the leading edge of the airfoil and decrease mildly over the airfoil surface up to the shock location then decrease sharply across the shock. As

expected, the skin friction coefficient is found to increase significantly with surface roughness height. Also the upstream movement of the shock at the upper surface and downstream movement at the lower surface are evident.

The total viscous drag is characterized by the viscous drag coefficient, $C_{D,v}$, which is basically the average of the skin friction coefficient over the airfoil surface. The variation of $C_{D,v}$ with increasing surface roughness heights for all the simulations performed is shown in Fig. 8. It is observed that the viscous drag coefficient increases monotonically with surface roughness height. However, at a fixed surface roughness height the $C_{D,v}$ values decrease with increasing freestream Mach number until M = 0.85. At M = 0.9 the viscous drag coefficient jumps up and is highest.

The pressure or form drag, the other significant part of the total drag for flow over airfoils, is characterized by the pressure drag coefficient, $C_{D,p}$. The variation of $C_{D,p}$ with surface roughness height for the various simulations is presented in Fig. 9. It is noticed that the pressure drag coefficient is rather insensitive to the roughness height. It drops slightly for $k_s = 0.5$ and remains almost invariant with increasing k_s for most cases. At a fixed k_s, however, $C_{D,p}$ increases significantly with the freestream Mach number. It should also be pointed out that the pressure drag coefficients are almost an order of magnitude larger than the viscous drag coefficient values. This indicates that the total drag is dominated by the pressure drag and the total drag coefficients will follow a similar trend.

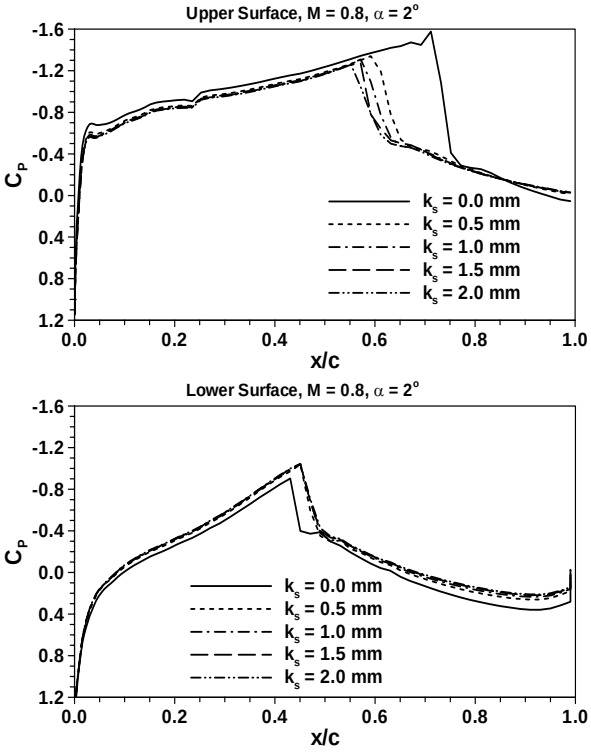

Fig 5. Pressure coefficient distribution along airfoil surface.

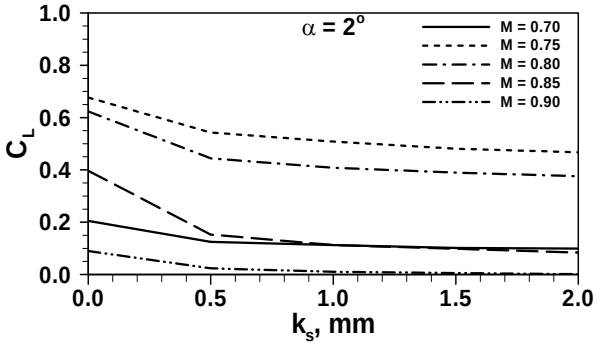

Fig 6. Variation of the lift coefficient with surface roughness height.

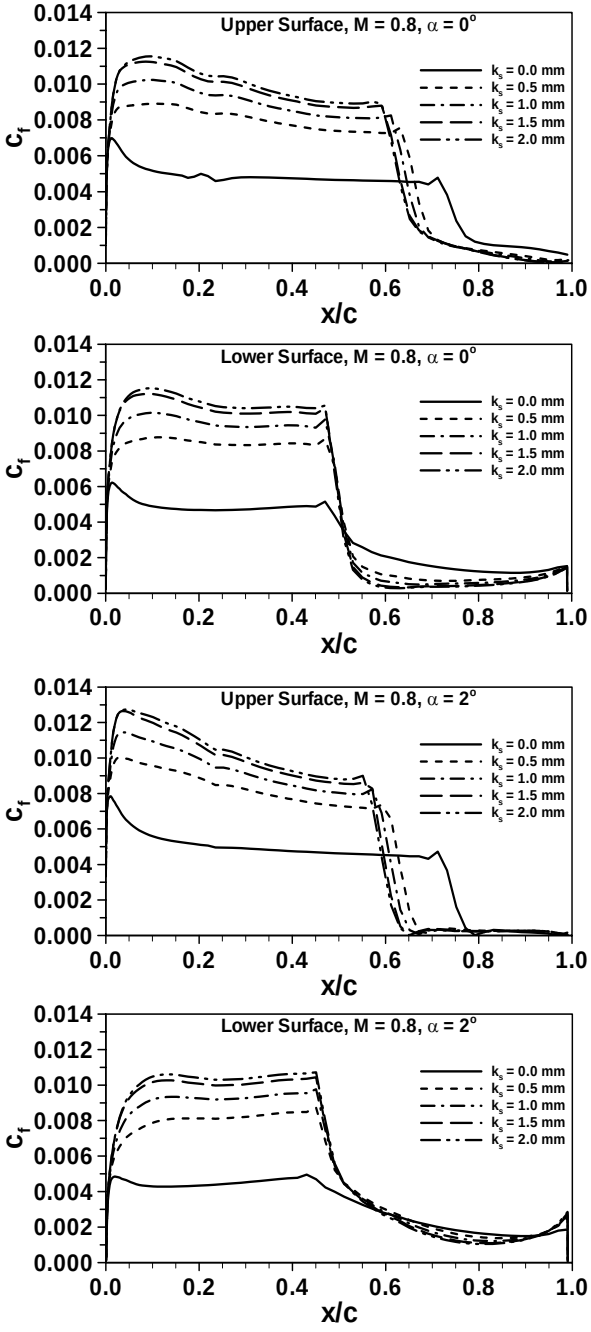

Fig 7. Distribution of the skin friction coefficient along the upper and lower surfaces of the airfoil.

The total drag coefficient, $C_D = C_{D,v} + C_{D,p}$ is plotted in Fig. 10 and it ascertains the above mentioned variation trend that the total drag is relatively insensitive to the surface roughness height for the range of flow parameters investigated in this study.

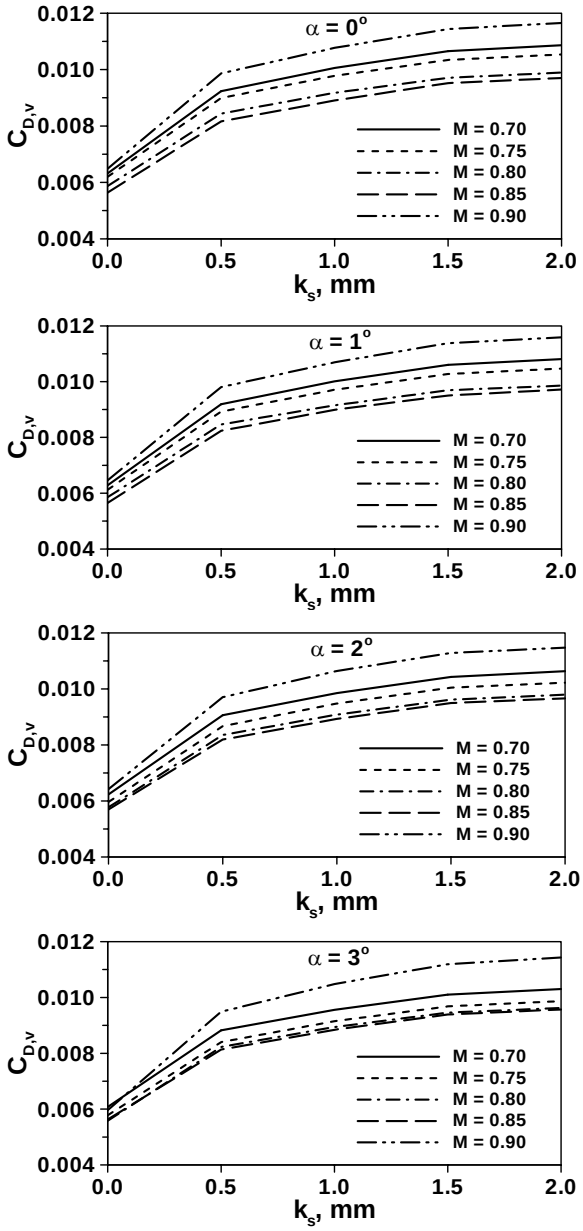

Fig 8. Variation of the viscous drag coefficient for the airfoil with surface roughness height.

4. CONCLUSIONS

Turbulent transonic flow over a two-dimensional RAE-2822 airfoil has been investigated numerically using the FLUENT CFD code in order to understand the effect of surface roughness on the performance of the airfoil. The two-equation $k-\omega$ turbulence model with enhanced wall treatment where the surface roughness is incorporated through the boundary condition for ω at the airfoil surface is used to calculate the eddy viscosity in the domain.

The transonic flow behavior has been successfully predicted by the code where the termination of the supersonic flow across a shock has been reasonably well predicted for a range of the important flow parameters such as the freestream Mach number, angle of attack, and the surface roughness height.

The effect of increasing surface roughness is manifested in the upstream movement of the shock location at the upper surface and downstream movement at the lower surface, increase in the skin friction coefficient and the viscous drag coefficient, and decrease in the lift coefficient. The pressure drag, which is an order of magnitude greater than the viscous drag, is not affected significantly by the surface roughness and hence the total drag is affected only slightly.

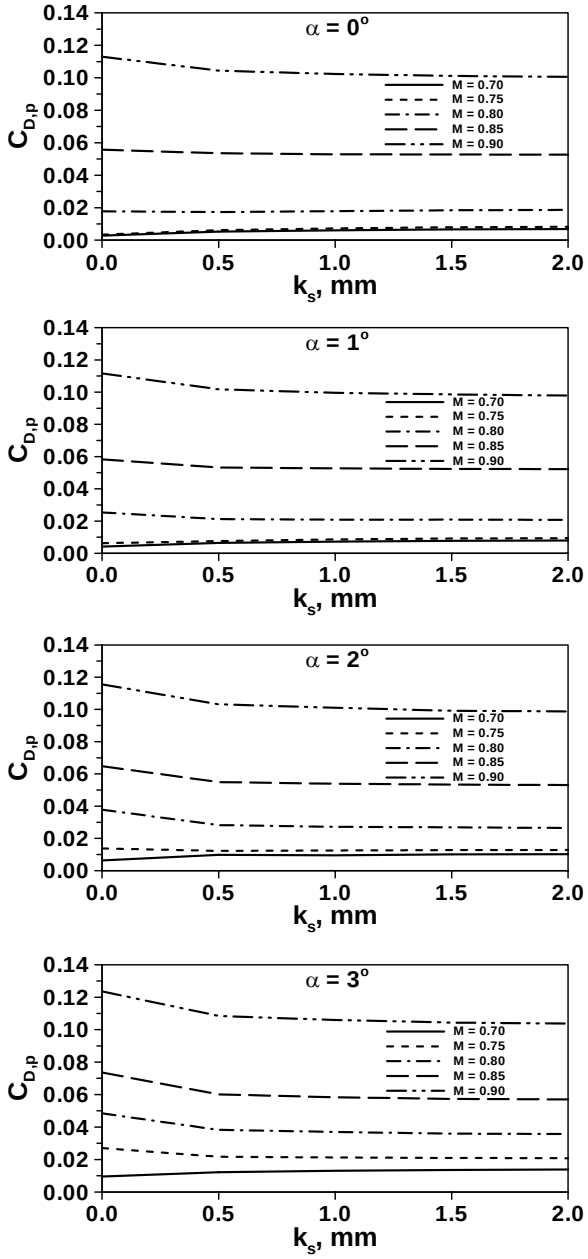

Fig 9. Variation of the pressure drag coefficient for the airfoil with surface roughness height.

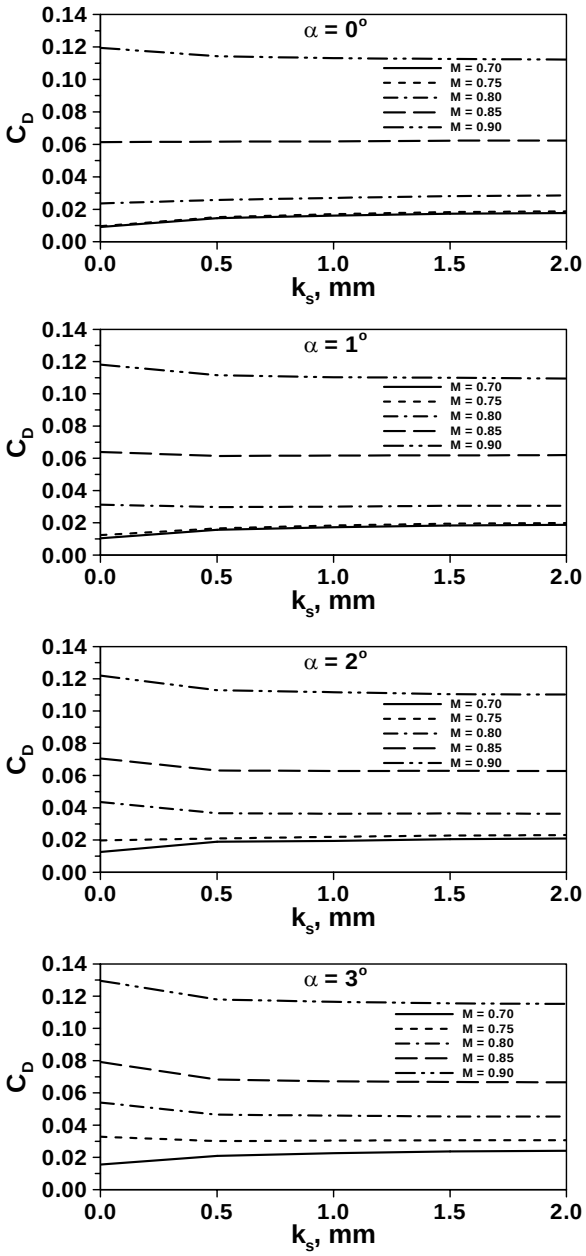

Fig 10. Variation of the total drag coefficient for the airfoil with surface roughness height.

5. REFERENCES

1. Ahmed, S. and Tannehill, J. C., 1992, "New Nonequilibrium Turbulence Model for Calculating Flows over Airfoils," AIAA Journal, 30:302-303.
2. Anderson, W. K. and Bonhaus, D. L., 1994, "An Implicit Upwind Algorithm for Computing Turbulent Flows on Unstructured Grids," Computers and Fluids, 23:1-21.
3. Jiang, Y. T., Damodaran, M., and Lee, K. H., 1997, "High-Resolution Finite Volume Computation of Turbulent Transonic Flow Past Airfoils," AIAA Journal, 35:1138-42.
4. Lien, F., and Kalitzin, G., 2001, "Computations of Transonic Flow with the v^2-f Turbulence Model," International Journal of Heat and Fluid Flow, 22:56-60.
5. Garbaruk, A., Shur, M., Strelets, M., and Spalart, P. R., 2003, "Numerical Study of Wind-Tunnel Walls Effects on Transonic Airfoil Flow," AIAA Journal, 41:1046-1054.
6. Cebeci, T., 1987, "Effects of Environmentally Imposed Roughness on Airfoil Performance," NASA CR-179639.
7. Mendonca, J. and Sharif, M. A. R., 2005, "Performance of Turbulence Models in the Computation of Transonic Flow over a Circular Arc Bump," AIAA 2005-4673, *35th AIAA Fluid Dynamics Conference and Exhibit*, 6-9 June 2005, Toronto, Ontario, Canada.
8. Wilcox, D. C., 2002, *Turbulence Modeling for CFD, Second Edition*.
9. Cook, T. J., McDonald, M. A., and Firmin, M. C. P., 1979, "Airfoil RAE-2822 Pressure Distributions and Boundary Layer Wake Measurements," AGARD Advisory Report 138, Sec. A6.

6. NOMENCLATURE

Symbol	Meaning	Unit
c	Chord length	(m)
C_D	Coefficient of drag	
$C_{D,v}$	Coefficient of viscous drag	
$C_{D,p}$	Coefficient of pressure drag	
c_f	Skin friction coefficient	
C_L	Coefficient of lift	
C_p	Pressure coefficient	
k_s	Sand-grain roughness height	(mm)
k_s^+	Dimensionless roughness height	
M	Mach number	
Re	Reynolds number	
U_∞	Freestream velocity	(m/s)
u_τ	Shear velocity	(m/s)
α	Angle of attack	(deg)
τ_w	Wall shear stress	(N m^{-2})
ρ_∞	Freestream density	(kg m^{-3})
ν	Kinematic viscosity	(m^2 s^{-1})